Original Article

The Spectrum of Radiological Findings of Rhino Orbital Cerebral Mucormycosis with Endoscopic and Histopathological Features in Patients with COVID 19: A Descriptive Study

Anjali B. Susan[1], Jerin Kuruvilla Varghese[1], Vivek Agarwal[1], Dimple Bhatia[1], Subhash Singla[1], Ashish Varghese[2], Preethi Paul[3]

Departments of [1]Radiology, [2]Otolaryngeology and [3]Pathology, Christian Medical College, Ludhiana, Punjab, India

Abstract

Background: There had been an increasing incidence of mucormycosis during the COVID-19 pandemic. **Aim:** This study evaluates the pattern of radiological imaging, endoscopic and histopathological features of rhino-orbital cerebral mucormycosis in patients with COVID-19 infection. **Materials and Methods:** The study included 31 patients with culture/biopsy-proven mucormycosis and COVID-19 infection from November 1, 2020, to December 31, 2021, in a single tertiary care centre. This study was approved by institutional ethics committee. Computed tomography (CT)/magnetic resonance imaging (MRI) images, endoscopic, and histopathological findings were retrospectively analyzed to look for the extent and pattern of disease. Statistical analysis was performed through descriptive statistics. **Results:** The imaging spectrum showed paranasal sinus involvement ($n = 31$; 100%), nasal involvement ($n = 14$; 45.16%), oral and palatal involvement ($n = 6$; 19.3%), deep neck/face space involvement ($n = 25$; 80.6%), orbital involvement ($n = 20$; 64.5%), vascular complications ($n = 9$; 29%), skull base involvement ($n = 12$; 38.7%), and cerebral involvement ($n = 10$; 32.2%). Endoscopy showed black necrotic tissue and slough mostly affecting middle turbinate, maxillary, and sphenoid sinuses. CT showed 100% sensitivity and specificity for the detection of sinonasal osseous erosion. Histopathology examination revealed mucormycosis as broad aseptate, predominantly 90° branching hyphae with macrophage and neutrophilic infiltration in 93.5%, granuloma in 61.3%, cavity formation in 48.4%, and angioinvasion in 77.4%. Diabetes mellitus was the predominant coexisting morbidity for mucormycosis. The mean time interval between COVID-19 diagnosis and mucormycosis was 18 days. **Conclusion:** CT revealed hyperdense contents within sinuses with osseous erosion; while MRI showed T2 hypointense, heterogeneously enhancing lesions with adjacent structural infiltration, orbital inflammation, cavernous sinus and internal carotid artery thrombosis, and intracranial complications such as infarct, hemorrhage, meningitis, and abscess. Neutrophilic infiltration and angioinvasion were predominant histopathological characteristics while necrosis with eschar formation was demonstrated through endoscopy.

Keywords: COVID, endoscopy, imaging, mucormycosis

Introduction

Novel coronavirus has emerged as a global pandemic since the first case was reported in Wuhan, China, in December 2019. Meanwhile, as we are dealing with the consequences of the outbreak in the world, another life-threatening infection mucormycosis has come into the picture. Primarily, a sinonasal disease, mucormycosis cases are triggered due to aggressive use of corticosteroids and immunosuppressants in the already immunocompromised COVID-19 patients with several predisposing factors such as diabetes, neutropenia, and cancer.[1] The clinical symptomatology on presentation is nonspecific including headache, low-grade fever, facial swelling, and orbital or paranasal sinus syndrome.[2] The occurrence of early visual loss would favour the diagnosis of rhino-orbital-cerebral mucormycosis over bacterial cavernous sinus thrombosis in which blindness is a much later finding.[2] Early diagnosis is vital due to its necrotising

Access this article online

Quick Response Code:

Website: www.njmonline.org

DOI: 10.4103/NJM.NJM_121_22

Address for correspondence: Dr. Vivek Agarwal, Gateway Terrace, CMC Campus, Ludhiana - 141 008, Punjab, India.
E-mail: vivekagarwal0004@gmail.com

How to cite this article: Susan AB, Varghese JK, Agarwal V, Bhatia D, Singla S, Varghese A, *et al*. The spectrum of radiological findings of rhino orbital cerebral mucormycosis with endoscopic and histopathological features in patients with COVID 19: A descriptive study. Niger J Med 2022;31:691-8.

Submitted: 22-Nov-2022 **Revised:** 22-Dec-2022
Accepted: 02-Jan-2023 **Published:** 28-Feb-2023

and angioinvasive nature causing it to spread to the deep face, orbit and brain through perivascular, perineural, and direct spread.[3,4] To maintain a high index of suspicion and early intervention is essential to bring down the morbidity and mortality associated with such cases, for which radiological imaging (computed tomography [CT] and magnetic resonance imaging [MRI]) in conjunction with histopathological and nasal endoscopic evaluation plays an essential role.

Objective

Evaluate pattern of radiological imaging, endoscopic and histopathological features of rhino-orbito-cerebral mucormycosis in COVID-19 patients.

Materials and Methods

This study was approved by the institutional review board and informed consent was waived by the review board as this was a retrospective study and the data were anonymised.

This was a retrospective study conducted in a single tertiary care centre in patients diagnosed with COVID-19 infection and mucormycosis, who underwent imaging in the department of radiology. A total of 45 patients had radiological imaging features of sinonasal disease from November 1, 2020, to December 31, 2021. Fourteen patients who were not laboratory confirmed for SARS-CoV-2 infection were excluded from the study.

Inclusion criteria

1. Patients who have undergone either or both modalities of cross-sectional imaging of the brain/orbit/paranasal sinuses (CT/MRI) and/or endoscopic evaluation from November 1, 2020, to December 31, 2021, with a radiological diagnosis of fungal sinusitis
2. Patients having biopsy/culture-proven diagnosis of mucormycosis irrespective of the presence of any other superadded fungal/bacterial infection
3. Patients who were laboratory-confirmed for SARS-COV-2 infection through reverse transcriptase-polymerase chain reaction.

Exclusion criteria

1. Sinusitis due to any other etiology such as bacterial/allergic sinusitis without mucormycosis infection.

Fourteen patients underwent both CT and MRI. Eleven patients underwent isolated CT and six patients underwent isolated MRI. CT scan was performed with Philips (Ingunity 128 slice) using paranasal (PNS) protocol with 120 kVp and 30 mA tube current. Intravenous contrast medium (low osmolar, nonionic, 300 mg/mL iodine content) was used at a dose of 2 ml/kg administered by a pressure injector. Head-and-neck MRI imaging was performed using 3 T Siemens (Magnetom Spectra Siemens) using 16 channel head coil. The imaging protocol included axial and coronal T1W, T2W, T2 FLAIR, diffusion-weighted imaging (DWI), and fat-suppressed postcontrast T1W sequences. Intravenous injection of meglumine gadoterate (0.1 mmol/kg) was given in contrast study. Images were retrospectively analysed by two radiologists for the site, the extent of involvement, and complications.

Image interpretation

Mucosal thickening of sinuses and nasal turbinates with or without osseous erosion on CT/MRI was recorded along with laterality and the presence of any complication. Density, signal intensity, and enhancement pattern of the sinuses were recorded. Any extra sinus involvement including face, oral cavity, palate, orbit, skull base, and deep spaces such as retro-maxillo-zygomatic space, masticator space, infratemporal fossa, parapharyngeal, and retropharyngeal space was assessed based on fat stranding or soft-tissue extension or abnormal enhancement pattern. On postcontrast CT/MRI superior ophthalmic artery, superior ophthalmic vein, cavernous sinuses, and internal carotid arteries were assessed for thrombosis in the presence of abnormal surrounding soft tissue. Orbital cellulitis was taken as intraconal/extraconal fat stranding with associated ≥1 bulky extraconal muscle. The presence of orbital apex involvement was seen as stranding or soft tissue in the optic canal/superior orbital fissure/ inferior orbital fissure. Complications such as an abscess and optic nerve involvement were also noted based on restricted diffusion on DWI and enhancement. Skull base extension was recorded through the foraminal extension of the disease. Patients with intracranial involvement were evaluated for dural enhancement, leptomeningeal enhancement, infarcts, intracerebral abscess, or hemorrhage.

The presence of necrosis, inflammation, and osseous erosion was assessed in the nasal cavity paranasal sinuses, and oral cavity through endoscopy. Biopsy taken from diseased tissue was analyzed for the presence of mucormycosis, the morphology of fungal hyphae, and any superadded infection.

Data were entered into Microsoft Excel Sheet and descriptive statistical analysis was performed.

Results

This was a cross-sectional retrospective study of patients (20 males and 11 females; mean age [range], 53.58 [23–76] years) with laboratory-confirmed COVID-19 infection and biopsy/culture-proven mucormycosis.

The predominant coexisting morbidity for mucormycosis was diabetes mellitus (n = 25; 80.6%). Steroid intake was seen in six patients (19.4%). The mean time interval between COVID-19 diagnosis and mucormycosis was 18 days.

Sinonasal and oral involvement of mucormycosis

CT showed predominantly sinuses (n = 25; 100%) and nasal involvement (n = 12; 48%). Maxillary sinus was most involved (n = 18; 92%). Most patients showed mucosal thickening isodense to the brain parenchyma in paranasal sinuses. Hyperdense contents were mostly demonstrated in maxillary and sphenoid sinuses. Detailed imaging findings

are given in Table 1. The oroantral fistula was noted in a single case. A single case demonstrated the involvement of the fossa of Rosenmuller which was earlier suspected as malignancy.

On MRI paranasal sinus involvement was observed in all patients (n = 20; 100%) and nasal involvement in 14 (70%) patients. Mucosal thickening in paranasal sinuses was T1 isointense to gray mater. T2 hypointense soft tissue was commonly observed within the sphenoid sinus and inferior turbinate. Eleven patients underwent a contrast MR study. The pattern of enhancement was predominantly heterogeneous (n = 8; 72%) with homogeneous enhancement observed in rest of them. Two (10%) cases showed "soap bubble appearance" of sinus. "Black turbinate sign" was noted in 2 (10%) cases. Five cases underwent contrast CT images. It showed a predominantly homogeneous enhancement pattern of paranasal sinuses (n = 4; 80%) and heterogeneous enhancement in a single case. Figures 1a-d and 2a-d show representative images.

Orbital, skull base, vascular and cerebral involvement of mucormycosis

The majority of patients had orbital cellulitis affecting intraconal/extraconal fat and extraocular muscles while isolated preseptal space involvement was noted in 6 (19.3%) cases. Three patients (9.7%) had proptosis and globe deformity with "guitar pick sign." Figures 3a-f and 4a show representative images.

The most common deep neck space affected was retro-maxillo-zygomatic space. Twelve (38.7%) cases showed foraminal extension with predominant involvement of sphenopalatine foramen, pterygomaxillary fissure, and pterygomaxillary fossa. Figures 4a-d and 5a-d show representative images.

Dural and leptomeningeal enhancement were the common intracranial finding in cerebral mucormycosis with cavernous sinus being the most frequently involved vascular structure.

Table 2 shows the detailed involvement of mucormycosis in the respective areas.

Endoscopy

Nasal endoscopy was done in all patients (n = 31) with simple debridement done in 14 (45.1%) and functional endoscopic

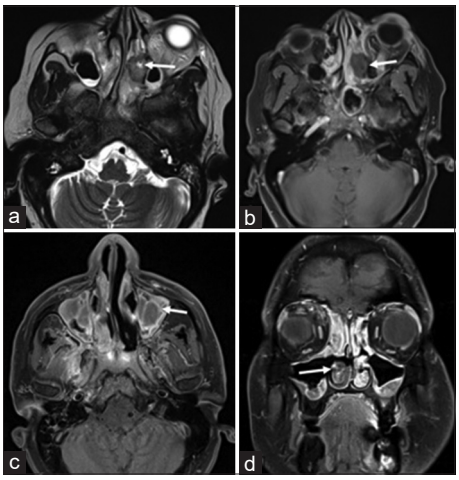

Figure 1: Mucormycosis with sinonasal involvement. (a) Axial T2 weighted image shows hypointense contents in left inferior turbinate (white arrow) suggestive of necrotic tissue, (b) Axial postcontrast fat suppressed T1 weighted image shows non enhancing necrotic tissue in left inferior turbinate (white arrow), (c) Axial postcontrast fat suppressed T1 weighted image shows complete opacification of maxillary sinus with septa enhancement giving "soap bubble appearance" in left maxillary sinus (white arrow), (d) Coronal post contrast fat suppressed T1 weighted image shows absent enhancement of right inferior turbinate: "Black turbinate sign" (white arrow)

Table 1: Imaging findings in paranasal sinuses and nasal cavity

Location	CT findings (n=25)			MRI findings (n=20)		
	Mucosal thickening, n (%)	Hyperdense contents, n (%)	Osseous erosion, n (%)	T1 isointense contents, n (%)	T2 hypointense contents, n (%)	Osseous erosion, n (%)
Maxillary sinus (right)	14 (56)	2 (8)	2 (8)	14 (70)	10 (50)	1 (5)
Maxillary sinus (left)	11 (44)	7 (28)	5 (20)	18 (90)	12 (48)	1 (5)
Ethmoid sinus (right)	16 (64)	0	3 (12)	18 (90)	13 (65)	2 (10)
Ethmoid sinus (left)	14 (56)	2 (8)	2 (8)	18 (90)	12 (48)	0
Sphenoid sinus (right)	12 (48)	6 (24)	0	17 (85)	14 (70)	1 (5)
Sphenoid sinus (left)	16 (64)	3 (12)	0	19 (25)	14 (70)	0
Frontal sinus	12 (48)	4 (16)	0	19 (25)	10 (50)	0
Superior turbinate (right)	4 (16)	0	0	5 (25)	4 (20)	0
Superior turbinate (left)	4 (16)	1 (4)	0	7 (28)	5 (25)	0
Middle turbinate (right)	6 (24)	0	0	8 (40)	6 (30)	0
Middle turbinate (left)	4 (16)	1 (4)	0	6 (30)	5 (25)	0
Inferior turbinate (right)	11 (44)	0	0	11 (55)	9 (32)	0
Inferior turbinate (left)	9 (36)	0	0	9 (32)	7 (28)	0
Palate	0	0	3 (12)	2 (10)	1 (5)	1 (5)
Septum	6 (24)	0	0	9 (32)	7 (28)	0

CT: Computed tomography, MRI: Magnetic resonance imaging

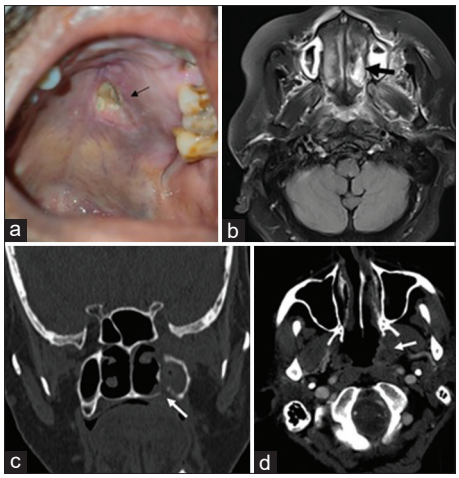

Figure 2: Mucormycosis with oral and palatal involvement. (a) Photograph image shows erosion of palate (black arrow), (b) Axial fat suppressed T2 weighted image shows left palatal involvement (white arrow) with inflammation in left masticator space, (c) Coronal CT image (bone window) shows erosion of medial and inferior wall of left maxillary sinus with oroantral fistula (white arrow), (d) Axial post contrast CT images shows peripherally enhancing soft tissue lesion in fossa of Rosenmullar (white arrow). CT: Computed tomography

Table 2: Details of other areas of involvement on imaging

Site of involvement	*n* (%)
Orbital involvement	
Involvement of intraconal/extraconal fat and extraconal muscles	20 (64.5)
Orbital apex	2 (6.45)
Intraorbital abscess	3 (9.68)
Optic neuritis	2 (6.45)
Proptosis and globe deformity	3 (9.68)
Preseptal space	6 (19.34)
Neck space involvement	
Retro-maxillo-zygomatic space	14 (45.16)
Masticator space	13 (41.93)
Retropharyngeal space	1 (3.22)
Parapharyngeal space	1 (3.22)
Premaxillary space	13 (41.93)
Intracranial involvement	
Infarct	3 (9.68)
Intracranial hemorrhage	2 (6.45)
Intracranial abscess	1 (3.22)
Dural enhancement	4 (12.90)
Leptomeningeal enhancement	4 (12.90)
Vascular involvement	
Cavernous sinus thrombosis	6 (19.35)
Internal carotid artery thrombosis	2 (6.45)
Superior ophthalmic vein thrombosis	1 (3.22)

sinus surgery (FESS) in 3 (9.6%). Blackish necrotic tissue, slough, and pus from diseased area were predominant endoscopic features. Three (9.4%) cases showed associated erosion of palate. There were also turbinates with pale mucosa suggesting reduced vascular supply. Necrotic changes were

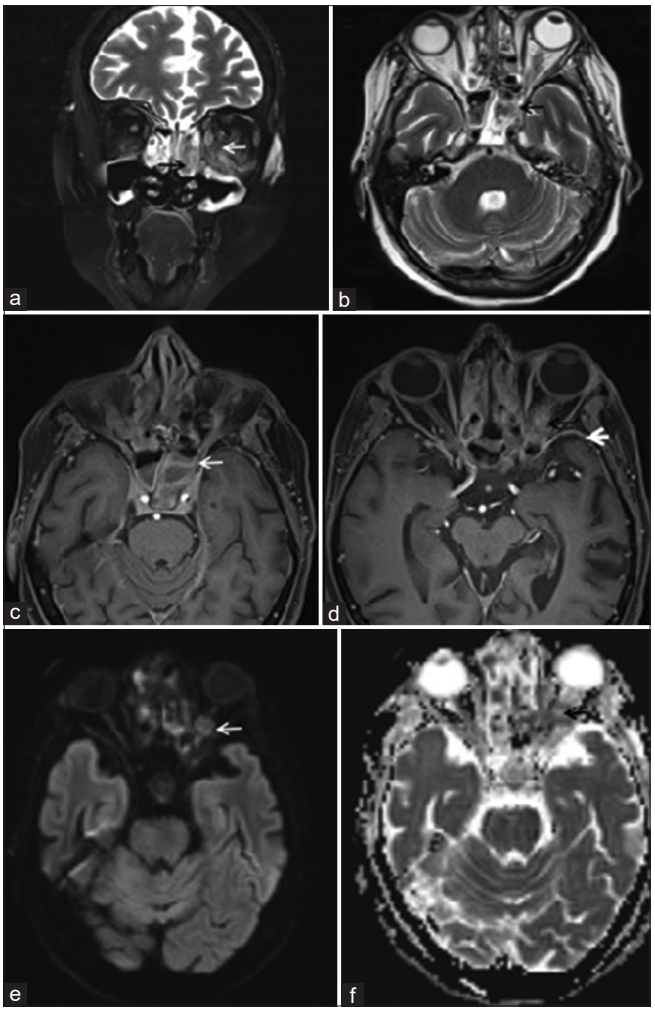

Figure 3: Mucormycosis with orbital involvement (optic neuritis with abscess). (a) Coronal fat suppressed T2 weighted image showing T2 hypointense (necrotic) contents in ethmoid air cells (black arrow) and hyperintense bulky extraocular muscles (white arrow) with intraconal and extraconal fat stranding, (b) Axial T2 weighted image demonstrates hypointense contents in sphenoid sinus with optic canal involvement (black arrow), (c and d) Axial postcontrast fat suppressed T1 weighted images showing peripheral enhancement along optic nerve at optic canal (white arrow) with ill-defined enhancing lesion in optic nerve (black arrow). There is adjacent dural enhancement along temporal convexity (thick white arrow), (e and f) Axial DWI and ADC images show peripheral restricted diffusion (white arrow) and corresponding ADC drop (black arrow) within lesion in optic nerve. DWI: Diffusion weighted imaging, ADC: Apparent diffusion coefficient

most commonly found within the middle turbinate, maxillary, and sphenoid sinuses. Detailed involvement of mucormycosis in nasal and paranasal sinuses is given in Table 3. Cerebrospinal fluid (CSF) leak due to erosion of the base of the skull was identified in three patients (9.6%). Alveolar process necrosis and erosion were seen in two patients (6.4%). Figure 6a and b show representative images.

Histopathology

Histopathological examination revealed broad aseptate branching hyphae in all cases (n = 31; 100%). The angle

Table 3: Endoscopic findings

Site	Inflammation Total number=31, *n* (%)	Necrosis Total number=31, *n* (%)	Erosion Total number=31, *n* (%)
Superior turbinate (right)	2 (6.45)	3 (9.68)	-
Superior turbinate (left)	2 (6.45)	-	-
Middle turbinate (right)	5 (16.13)	10 (32.26)	-
Middle turbinate (left)	7 (22.58)	8 (25.81)	-
Inferior turbinate (right)	1 (3.23)	4 (12.90)	-
Inferior turbinate (left)	5 (16.13)	7 (22.58)	-
Maxillary sinus (right)	5 (16.13)	2 (6.45)	2 (6.45)
Maxillary sinus (left)	5 (16.13)	7 (22.58)	5 (16.13)
Ethmoid sinus (right)	-	3 (9.68)	3 (9.68)
Ethmoid sinus (left)	1 (3.23)	2 (6.45)	2 (6.45)
Sphenoid sinus (right)	1 (3.23)	5 (16.13)	-
Sphenoid sinus (left)	1 (3.23)	2 (6.45)	-
Oral cavity	-	2 (6.45)	-
Palate	1 (3.23)	3 (9.68)	3 (9.68)
Septum	2 (6.45)	5 (16.13)	-
Pterygopalatine fossa	-	-	1 (3.23)

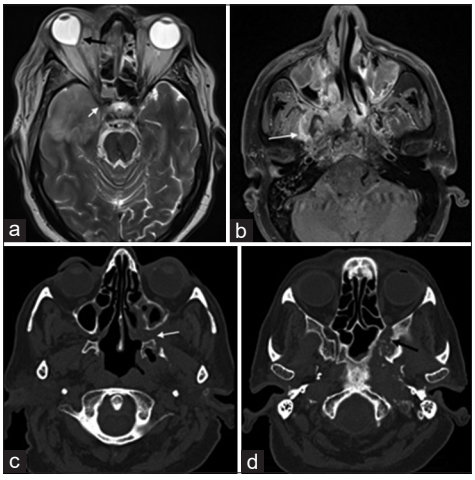

Figure 4: Mucormycosis with foraminal, deep space and skull base involvement. (a) Axial T2 weighted image shows hypointense lesion in right optic canal (white arrow) with tenting of posterior globe: "guitar pick sign" (black arrow), (b) Axial postcontrast fat suppressed T1 weighted image shows heterogeneously enhancing ill-defined lesion involving the right masticator space with involvement of sphenoid bone and clivus (white arrow), (c) Axial CT image shows soft tissue within left greater palatine foramen (white arrow) extending from left ethmoid air cells. (d) Axial CT images shows erosion of left greater wing of sphenoid and involvement of left pterygoid canal (black arrow). CT: Computed tomography

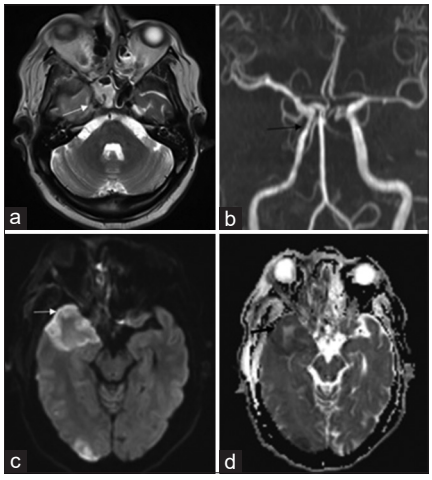

Figure 5: Mucormycosis with vascular and intracranial involvement. (a) Axial T2 weighted image shows mucosal thickening in sphenoid sinus with T2 hypointense lesion (necrotic tissue) involving right cavernous sinus with associated narrowing of cavernous segment of right internal carotid artery (white arrow), (b) Black arrow shows the narrowed and irregular cavernous and supraclinoid segment of right internal carotid artery, (c and d) Axial DWI and ADC images show restricted diffusion in right temporal and occipital lobe with ADC drop concerning for infarcts. DWI: Diffusion weighted imaging, ADC: Apparent diffusion coefficient, TOF: Time of flight

of branching was found to be 90° in the majority (n = 30; 96.7%). Macrophage and neutrophil infiltration were noted predominantly (n = 29; 93.5%) while granulations were identified in 19 (61.3%) cases. Cavities were demonstrated in 15 (48.4%) cases and angioinvasion was observed in 24 (77.4%) cases. Seven (22.5%) cases had superadded candida infection and 4 (12.9%) cases had associated aspergillosis.

Figure 6c and d show representative images.

Discussion

In this study, more than half of the patients were male and middle aged. This demographic profile was comparable to a study by Ramaswami *et al*. which included previously treated COVID patients with mucormycosis where two-thirds of patients were males and ages ranged between 38 and 55 years.[3] Our study showed that the mean time interval of development of mucormycosis following COVID infection to be 18 days which was similar to the study by Jain *et al*.

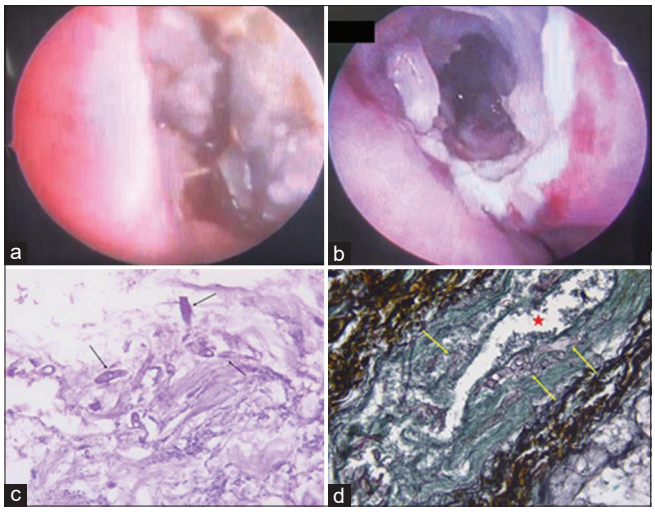

Figure 6: Endoscopy and histopathology demonstrating mucormycosis. (a) Endoscopic image shows blackish necrotic tissue in inferior turbinate (b) Endoscopic image shows erythematous nasal mucosa with slough and ulceration, (c) Biopsy from hard palate showing invasive broad aseptate fungal hyphae (arrows) within necrotic tissues (H and E, ×400), (d) Hard palate biopsy showing angioinvasive broad aseptate fungal hyphae (yellow arrows) within vessel wall (red star), Gomori's silver methenamine stain (×400)

and systemic review analysis by Nagalli and Kikkeri.[5,6] This suggests an increased risk of mucormycosis in patients with COVID infection.

Mucormycosis primarily affects immunocompromised individuals with pre-existing comorbidities such as diabetes mellitus with poor glycemic control, malignancies, and corticosteroid or immunosuppressant intake. A systemic review study by Singh *et al*. reported that 80% of patients with diabetes mellitus and 76.3% with corticosteroid intake developed mucormycosis following COVID-19 infection.[7] Nagalli and Kikkeri reported diabetes mellitus to be a common comorbidity (77.1%). The steroid intake was seen in 55.2% of cases. Other comorbidities such as hypertension and renal disease were observed in 29.5% and 14.3%, respectively.[5] Our study reflected similar findings with coexisting predisposing factors in most cases as diabetes mellitus (80.6%) followed by hypertension (32.2%). Steroid intake was noted only in 19.4%.

Mucormycosis infection is usually by inhalation of spores of the Phycomycetes fungi, most commonly belonging to the genera Mucor, Rhizopus and Absidia. It is characterised by angioinvasion which leads to deeper structural involvement, thrombosis, and tissue necrosis. Since airway epithelial damage and immune dysfunctions are seen in COVID-19 infection, patients are predisposed to extensive involvement of mucormycosis.[8-11] In our study, mucormycosis affected the nasal cavity (45.16%) and sinuses (100.0%) in the majority of patients with osseous destruction in 38.7% of patients. There was a significant extension to deep spaces of the neck (80.6%) and orbits (64.5%). Cerebral involvement was seen in 32.2%. Similar findings were noted in a systematic review study by Singh *et al*. with predominant sinonasal (88.9%) and rhino-orbital (56.7%) involvement of mucormycosis with cerebral involvement in 22.2% of patients.[7] Pal *et al*. reported rhino-orbital mucormycosis to be the most common (42%), followed by rhino-orbito-cerebral mucormycosis (24%).[12] Nagalli and Kikkeri reported cavernous sinus involvement in 14.4% which reflected findings similar to our study.[5]

The CT appearance of mycetoma is a hyperdense sinus with internal calcification. There can be thickened sclerosed sinus walls or thinned out and expanded walls in case of chronic sinusitis.[15] Mucormycosis is an aggressive disease which results in adjacent wall erosion and extension into retroantral fat seen as fat stranding or hypodense lesion. They may show homogeneous or heterogeneous enhancement.[13]

From a single-center study by Joshi *et al*., the maxillary sinus was most frequently sinus and 80% had osseous erosion. Hyperdense contents in sinuses were noted in 24% of cases which were similar to our study.[13] According to Singhal *et al*. maxillary and ethmoid sinuses were predominantly involved and had mucosal thickening. Only a few cases showed osseous erosion in the sinus wall and the majority showed palatal and maxillary alveolar process erosion. CT showed predominantly mild heterogeneous enhancement. Retroantral involvement (72%) was a frequent finding and the mild enhancement of hypodense soft tissue. They also reported intense homogeneous enhancement in most cases (43%) on MRI which was similar to findings from our study.[14] Intense or heterogeneous enhancement was noted in CT in 44% of cases according to Singhal *et al*. In our study, only 5 (20%) cases underwent contrast CT imaging which showed predominantly peripheral homogeneous enhancement of sinus mucosa.

The MRI appearances of the mucormycosis showed predominantly hypointense to isointense signal in all sequences, as well as variable enhancement pattern on postcontrast images, ranging from homogeneous to heterogeneous to no enhancement at all, as observed by Herrera *et al*.[2] However, a spectrum of imaging appearances was noted, ranging from simple inflammatory mucosal thickening of the sinus walls showing T1 hypointense and T2 hyperintense signals and on the other hand, intervening areas of T2 hypointense signals were seen within the areas of mucosal thickening to suggest the presence of fungal elements, as described in the study by Desai *et al*.[15,16] However, Lone *et al*. described MRI features to be T2 hyperintense diffusely infiltrating lesion extending from T2 hyperintense sinus wall into orbital apex and intracranial structures along with narrowed internal carotid artery and associated slow flow signal changes within it.[17] The wide spectrum of MRI appearances opens up an avenue for further exploration with imaging and their corresponding correlation to nasal endoscopy. Our study showed a similar pattern of involvement as described in these prior studies, with the areas of direct infiltration by the fungal hyphae showing a T2 hypointense signal and corresponding areas of heterogeneous enhancement observed within paranasal sinuses.

In addition to the involved paranasal sinuses, the portions of extrasinus involvement may show evidence of restricted diffusion on DWI images with a signal drop on apparent diffusion coefficient (ADC) maps.[17] Permeative destruction of the sinus wall may be seen, as well as that of adjacent osseous structures.[18] "Black turbinate sign" is a specific imaging sign described in sinonasal mucormycosis, whereby there is complete nonenhancement of the devitalized and necrotic sinonasal mucosa.[18] Our study showed 6.4% (n = 2) cases with a black turbinate sign.

Another novel imaging sign that was described is the "soap bubble appearance sign" which was observed in complete maxillary sinus opacification, where there is heterogeneous postcontrast enhancement of the septae and nonenhancement of the background sinus.[19] Our study showed two such cases.

The pattern of orbital involvement may be two-fold; intraorbital extension may manifest as T2 hypointense signal of protruding soft tissue from the sinus walls, and heterogeneous postcontrast enhancement with or without osseous destruction. Inflammatory changes are seen in the form of stranding of the extraocular muscles and intraconal fat as well as abnormally enhancing soft tissue at the orbital apex causing mass effect on the optic nerve. There can be abnormal enhancement of the optic nerve sheath or nerve.[16] A variable degree of proptosis may be seen. In severe proptosis, there can be tenting of the posterior globe ("guitar pick sign"). Our study demonstrated two cases with this sign. DWI images play an important role in the detection of optic nerve infarctions, as well as the differentiation of orbital cellulitis and abscess.[18] All these patterns were demonstrated in our study.

Retro-maxillo-zygomatic space was the most commonly affected deep neck space followed by masticator space and premaxillary space. The involvement of pterygopalatine fossa had led to extension into other compartments through the sphenopalatine foramen, pterygopalatine foramen, and pterygomaxillary fissure as reported by few cases series.[20-23] The extensive disease showed skull base involvement with thickening and narrowing of cranial foramina. The angioinvasive nature of the disease led to the intracranial extension and skull base osteomyelitis. One of the earliest indicators of intracranial involvement is abnormal dural enhancement and leptomeningeal enhancement. Perineural or orbital apex extension may lead to the involvement of the cavernous sinus. Cavernous sinus thrombosis is very well demonstrated on postcontrast 3D T1-weighted images in the form of abnormal enhancement and asymmetric bulging, with iso to hypointense signal on T2-weighted images.[16] Another intracranial manifestation observed is lacunar cortical territory watershed infarcts, observed as areas of restricted diffusion on DWI images, with a signal drop on ADC maps.[17] Perineural spread of disease may occur through the branches of the trigeminal nerve or Vidian nerve, seen in the form of abnormal sheet-like enhancement along the involving nerve or its branches and enlargement of the bulk of the nerve as well as obliteration of the foraminal fat.[16,18] Advanced intracranial involvement may be seen in the form of cerebritis and abscess formation, characterised by T1/T2 hypointense signal and peripheral postcontrast enhancement of the involved areas.[16] DWI sequences in fungal abscesses show evidence of restricted diffusion of the abscess walls and intracavitary projections and sparing of the core of the abscess.[18] Our study showed few cases of intracranial involvement demonstrating these findings.

Nasal endoscopy plays an important role to initiate the management by helping to arrive at a provisional diagnosis and assess the extent of the disease. This is achieved by examination of the nasal mucosa and turbinates for any discoloration, ulceration, or eschar formation, which may act as diagnostic clues.[24] Kumar *et al*. observed that the majority of mucormycosis cases had blackish crusts filling the nasal cavity and middle meatal region.[24] Few of the cases also had erosions of the hard palate. In cases with ischemia, there is whitish discoloration of the mucosa.[25] However, a major limitation of nasal endoscopy is the inability to assess the extent of the disease beyond the confines of the nasal cavity, where imaging plays an essential role.[26] FESS is lauded as a competent technique to control the disease process in its early and well-circumscribed stage.[27] Our FESS and endoscopy data showed necrotic discoloration, ulceration, or eschar formation in 30.6% (n = 64) of the sites observed in these patients. Furthermore, endoscopically proven osseous erosions were seen in 8 cases (25.8%), the hard palate being the commonest site. Alveolar processes were eroded in 2 patients and erosion of the cribriform plate and ethmoid sinus resulted in CSF leak in 3 patients.

Direct microscopy examination with potassium hydroxide helps in the identification of the fungus. Species identification and diagnosis are done through histopathological examination with hematoxylin and eosin (H and E), periodic acid–Schiff or Grocott's Methenamine silver. Mucormycosis has broad aseptate/pauci-septate hyphae with width of 6–25 μ. The angle of branching ranges from 45° to 90°. It shows necrosis, angioinvasion, perineural invasion, and neutrophilic infiltration. The chronic lesions are identified though the presence of pyogranulomatous inflammation, giant cells, or through Splendore–Hoeppli phenomenon. The demonstration of sporangiospores within the sporangia helps in differentiating mucormycosis from *Aspergillus*.[28] In a study by Jain *et al*., all patients showed broad aseptate branching fungal hyphae with inflammation. There were predominantly neutrophil infiltrates noted in 62% of cases.[6] All cases reported by Jain *et al*. had a ribbon pattern with irregular 90° branching. All cases showed variable degrees of angioinvasion. All cases showed necrosis with more than 50% of tissue involvement noted in 58% of cases. There was the single case that demonstrated granuloma around the fungus.[6] Our study showed a similar morphological appearance; however, had predominantly neutrophilic and macrophagic infiltration and granuloma in 61.3% patients. Twenty-four (77.4%) cases showed angioinvasion with none of them showing perineural invasion.

Strengths and limitations

High mortality and morbidity in COVID patients with associated rhino-orbito-cerebral mucormycosis and retrospective nature of the study limited uniformity in imaging. Despite the smaller sample population, most of the complications of the disease process were demonstrated including specific imaging signs.

Conclusion

The study showed advanced stages of the disease with extensive sinonasal, deep neck space, orbital involvement, intracranial and vascular complications within a limited duration following COVID-19 diagnosis. CT revealed hyperdense contents within the sinuses with associated osseous erosion; while MRI showed T2 hypointense, predominantly heterogeneously enhancing lesion with adjacent structural infiltration predominantly retro-zygomaticomaxillary space, associated orbital inflammation, cavernous sinus and internal carotid artery thrombosis, resultant intracranial complications such as infarct, hemorrhage, meningitis, and abscess. Neutrophilic infiltration and angioinvasion were predominant histopathological characteristics while necrosis with eschar formation of involved areas was demonstrated through endoscopy.

Financial support and sponsorship

Nil.

Conflicts of interest

There are no conflicts of interest.

References

1. Raut A, Huy NT. Rising incidence of mucormycosis in patients with COVID-19: Another challenge for India amidst the second wave? Lancet Respir Med 2021;9:e77.
2. Herrera DA, Dublin AB, Ormsby EL, Aminpour S, Howell LP. Imaging findings of rhinocerebral mucormycosis. Skull Base 2009;19:117-25.
3. Ramaswami A, Sahu AK, Kumar A, Suresh S, Nair A, Gupta D, *et al.* COVID-19-associated mucormycosis presenting to the emergency department-an observational study of 70 patients. QJM 2021;114:464-70.
4. Al Hassan F, Aljahli M, Molani F, Almomen A. Rhino-orbito-cerebral mucormycosis in patients with uncontrolled diabetes: A case series. Int J Surg Case Rep 2020;73:324-7.
5. Nagalli S, Kikkeri NS. Mucormycosis in COVID-19: A systematic review of literature. Infez Med 2021;29:504-12.
6. Jain K, Surana A, Choudhary TS, Vaidya S, Nandedkar S, Purohit M. Clinical and histology features as predictor of severity of mucormycosis in post-COVID-19 patients: An experience from a rural tertiary setting in Central India. SAGE Open Med 2022;10:20503121221074784. doi:10.1177/20503121221074785.
7. Singh AK, Singh R, Joshi SR, Misra A. Mucormycosis in COVID-19: A systematic review of cases reported worldwide and in India. Diabetes Metab Syndr 2021;15:102146.
8. Petrikkos G, Skiada A, Lortholary O, Roilides E, Walsh TJ, Kontoyiannis DP. Epidemiology and clinical manifestations of mucormycosis. Clin Infect Dis 2012;54 Suppl 1:S23-34.
9. Parasher A. COVID-19: Current understanding of its pathophysiology, clinical presentation and treatment. Postgrad Med J 2021;97:312-20.
10. Therakathu J, Prabhu S, Irodi A, Sudhakar SV, Yadav VK, Rupa V. Imaging features of rhinocerebral mucormycosis: A study of 43 patients. Egypt J Radiol Nucl Med 2018;49:447-52.
11. Ibrahim AS, Spellberg B, Walsh TJ, Kontoyiannis DP. Pathogenesis of mucormycosis. Clin Infect Dis 2012;54 Suppl 1:S16-22
12. Pal R, Singh B, Bhadada SK, Banerjee M, Bhogal RS, Hage N, *et al.* COVID-19-associated mucormycosis: An updated systematic review of literature. Mycoses 2021;64:1452-9.
13. Joshi AR, Muthe MM, Patankar SH, Athawale A, Achhapalia Y. CT and MRI findings of invasive mucormycosis in the setting of COVID-19: Experience from a single Center in India. AJR Am J Roentgenol 2021;217:1431-2.
14. Singhal A, Jain S, Sharma S, Kottiyath VC, Khandelwal G. A multicentric observational study of imaging findings in COVID-19-related rhino-orbito-cerebral mucormycosis: A new Pandora's Box. Egypt J Radiol Nucl Med 2021;52:258.
15. The Opacified Paranasal Sinus: Approach and Differential. Available from: https://appliedradiology.com/Communities/Artificial-Intelligence/the-opacified-paranasal-sinus-approach-and-differential [Last accessed on 2022 May 3]
16. Desai SM, Gujarathi-Saraf A, Agarwal EA. Imaging findings using a combined MRI/CT protocol to identify the "entire iceberg" in post-COVID-19 mucormycosis presenting clinically as only "the tip". Clin Radiol 2021;76:784.e27-784.e33.
17. Lone PA, Wani NA, Jehangir M. Rhino-orbito-cerebral mucormycosis: Magnetic resonance imaging. Indian J Otol 2015;21:215.
18. Kondapavuluri SK, Anchala VK, Bandlapalli S, Gorantla R, Danaboyina AR, Kondapavuluri BK, *et al.* Spectrum of MR imaging findings of sinonasal mucormycosis in post COVID-19 patients. BJR 2021;94:20210648. doi:10.1259/bjr.20210648.
19. Metwally MI, Mobashir M, Sweed AH, Mahmoud SM, Hassan AG, ElKashishy K, *et al.* Post COVID-19 head and neck mucormycosis: MR imaging spectrum and staging. Acad Radiol 2022;29:674-84.
20. Roushdy T, Hamid E. A case series of post COVID-19 mucormycosis-a neurological prospective. Egypt J Neurol Psychiatr Neurosurg 2021;57:100.
21. Eswaran S, Balan SK, Saravanam PK. Acute fulminant mucormycosis triggered by COVID 19 infection in a young patient. Indian J Otolaryngol Head Neck Surg 2022;74:3442-6.
22. Werthman-Ehrenreich A. Mucormycosis with orbital compartment syndrome in a patient with COVID-19. Am J Emerg Med 2021;42:264.e5-264.e8.
23. Awal SS, Biswas SS, Awal SK. Rhino-orbital mucormycosis in COVID-19 patients – A new threat? Egypt J Radiol Nucl Med 2021;52:152.
24. Kumar RA, John NM, Ramya B, Satish HS. Management of sinonasal mucormycosis at a tertiary care Center: Our experience. Int J Clin Rhinol 2021;12:52-6.
25. Singh VP, Bansal C, Kaintura M. Sinonasal mucormycosis: A to Z. Indian J Otolaryngol Head Neck Surg 2019;71:1962-71.
26. Shaikh N, Shakrawal N, Chouhan M, Solanki B. Diagnostic accuracy of nasal endoscopy and contrast magnetic resonance imaging in COVID-19 associated mucormycosis (CAM). Preprints 2021. doi:10.22541/au.163465369.96614812/v1.
27. Alobid I, Bernal M, Calvo C, Vilaseca I, Berenguer J, Alós L. Treatment of rhinocerebral mucormycosis by combination of endoscopic sinus debridement and amphotericin B. Am J Rhinol 2001;15:327-31.
28. Sood A, Nayyar V, Mishra D, Kakkar A, Priya H. Post-COVID mucormycosis: Ascertainment of the pathological diagnostic approach. J Oral Maxillofac Pathol 2021;25:219-22.